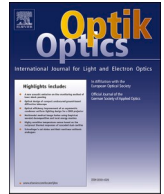




ELSEVIER

Contents lists available at ScienceDirect

Optik

journal homepage: www.elsevier.com/locate/ijleo

Original research article

Research on high performance support technology of space-based large aperture mirror

Wang Kejun^{a,*}, Dong Jihong^a, Zhao Yang^{a,b}, Chi Chunyan^c, Jiang Ping^a, Wang Xiaoyu^a

^a Chang Chun Institute of Optics, Fine Mechanics and Physics, Chinese Academy of Sciences, Changchun 130033, China

^b University of Chinese Academy of Sciences, Beijing, 100049, China

^c Jilin Jianzhu University, Changchun 130118, China

ARTICLE INFO

Keywords:

Space remote sensor
The back support
The simulation analysis
Surface shape error test
Mechanical test
Metering assembly

ABSTRACT

A three-point back support structure including cone sleeve, flexible structure and adjustable pad is designed for the space-based mirror support to meet the requirements of small surface shape error, high supporting reliability and stability, of which in-depth study on support principle and engineering realization is conducted in this paper. The error sources which influence the surface shape error of the mirror subassembly with three-point back support is summarized. The mechanism of surface shape variation caused by various error sources is studied. The support structure with high stiffness for alleviating the surface shape error caused by various error sources is designed, which can increase the fundamental frequency of mirror subassembly and protect it from yield failure under the condition of dynamic load. Firstly, the static and dynamic simulation of the three-point back support structure model is carried out by means of finite element analysis. Then the dynamic and partial static experiments are performed using aluminum mirror and actual supporting structure. The results show that the surface shape error of mirror with the three-point support structure is superior to $\lambda/80$ ($\lambda = 632.8$ nm), the displacement of mirror is smaller than 0.015 mm, the inclination angle is smaller than $2''$, the mass of the mirror subassembly is smaller than 310 kg. The mirror subassembly has a reasonable modal distribution, the fundamental frequency is 128 Hz, which is much higher than the requirement of 120 Hz. The maximum magnification of the mirror assembly excited by the sinusoidal vibration and the random vibration is 2.51 and the maximum stress is 286 MPa under the same working condition, which is much lower than the yield limit of the selected material. A kind of segmented metering assembly method is formed and applied to make sure 2 m space-based large-aperture mirror has lower surface shape error according to the theoretical research results in this paper which the surface shape error of the space-based large-aperture mirror supported by three-point on the back which optical axis is in the horizontal direction in test, installation and adjustment is very sensitive to the deviation between rotating shaft of flexible structure and the neutral plane of the mirror in the direction of the optical axis.

* Corresponding author.

E-mail address: wangkejun@ciomp.ac.cn (K. Wang).

<https://doi.org/10.1016/j.ijleo.2020.165929>

Received 12 August 2020; Accepted 30 October 2020

Available online 4 November 2020

0030-4026/© 2020 Published by Elsevier GmbH.

1. Introduction

The mirror subassembly is one of the most important components in the space remote sensor of which imaging quality is determined by the supporting performance of the mirror's support structure. According to the domestic and abroad research, the supporting modes of space-based large-aperture mirror include three categories that are passive supporting mode, gravity unloading mode and active optical mode. The passive support mode is a traditional one that has high reliability and stability. However, the larger the diameter of the mirror is, the more complicated the structure of passive support mode is. The active optics mode is a new one that can correct the mirror surface shape error by adjusting the driving force in real time. But the shortcoming of active optics mode is not reliable because of its complicated structure. Gravity unloading mode simulate the on-orbit environment to ensure the low surface shape error during installation procedure on the ground by means of applying to a certain number of gravity unloading devices to the mirror. The surface shape error remains unchanged when the gravity unloading devices are disconnected under the on-orbit working condition. It is hard for the gravity unloading mode to accurate the unloading gravity and make sure the unloading residual small enough. Active optical mode and gravity unloading mode are mostly used to support large-size mirrors with a diameter more than 1 m. Mirrors with a diameter less than 1 m are more likely to adopt passive support mode. Mirrors with a diameter between 1 m and 3 m also can adopt passive support mode. The specific support ways of passive support mode include peripheral support, back support and composite support, etc [1–4].

In this paper, the author focus on in-depth analysis on the supporting principle and realization approach in engineering of space-based mirror support. The error sources of three-point back support are summarized and the methods controlling each error source are found out. The feasibility of the support structure on a 2 m-aperture mirror subassembly is confirmed by means of simulation and experiment method. A kind of segmented metering assembly method is formed according to the theoretical research results in this paper which the surface shape error of the space-based large-aperture mirror supported by three-point on the back which optical axis is in the horizontal direction in test, installation and adjustment is very sensitive to the deviation between rotating shaft of flexible structure and the neutral plane of the mirror in the direction of the optical axis.

2. Principle of mirror support

2.1. Target of mirror support

Two important goals should be achieved to guarantee the supporting stability of the mirror. One is to determine the spacial orientation of the mirror in the optical system. Hence, the mirror should be regarded as a rigid body and restrained 6 DOF according to kinematics of mechanism. The supporting structure in such situation should be indeterminate or statically indeterminate. The other one is to ensure the stiffness of the mirror body so that a smaller mirror surface shape error will be obtained. Therefore, the mirror should be regarded as an elastomer to reduce its deformation by increasing the specific stiffness of the mirror or increasing the number of support points [5].

2.2. Principle of three-point back support

The mirror has 6 DOF that is the displacement along the X, Y and Z axes and the rotations around them respectively. If every possible motion of the mirror is individually constrained by a single point of contact, the mirror is limited by determinate constraint. If a possible motion of the mirror is constrained by several ways at the same time, the mirror is limited by statically indeterminate constraint, which result in the deformation of mirror due to the additional force from support structure [6].

The mirror with 3-point back support actually is a hyperstatic structure because of the surface contact in every support. Therefore, the mirror body will produce non-free deformation when the mirror subassembly is subjected to the effects of gravity load, temperature load and assembly error, which is unexpected.

The proper flexible structure is introduced to the support structure and arranged reasonably to absorb the deformation energy caused by additional forces. Hence, the surface shape deformation of mirror will be relieved and the spacial orientation of the mirror also come true.

3. Design and optimization

3.1. Induction of error sources

Generally, five important targets for mirror design include mirror surface shape error, mirror displacement, inclination angle, mass and dynamic performance. They should be minimized in the premise of ensuring the performances indexes of the mirror subassembly.

The mirror surface shape error is the deformation compared to the ideal surface shape, which is depend on the stiffness of the mirror, the number and the position of support points, and the type of support structure.

The mirror displacement is the linear offset of the mirror from its ideal position when the mirror subassembly sustains gravity load, which is depend on the stiffness of support structure. The smaller the stiffness of the support structure is, the larger the mirror displacement will be.

The inclination angle is the angle deviation of mirror to its ideal position when the mirror subassembly sustains gravity load, which is depend on the stiffness of support structure and support position in the direction of optical axis.

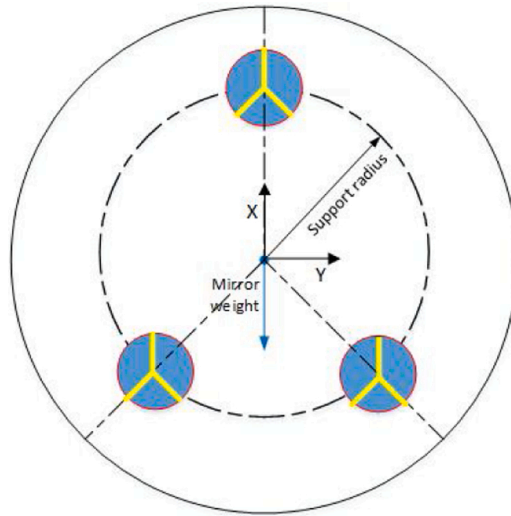


Fig. 1. Mirror assembly with gravity load.

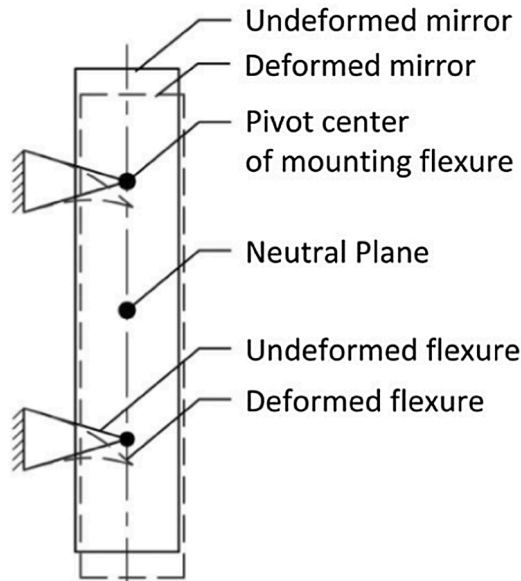


Fig. 2. Optimal assembly position of flexible structure and mirror.

The greater the mass of mirror subassembly is, the higher the launch cost of the space remote sensor will be.

Dynamic performance refers to the dynamic stress and dynamic response, which depend on the stiffness of each structure part of the mirror subassembly. The fundamental frequency of mirror subassembly can be improved by increasing the stiffness of each structure part in the mirror subassembly. However, the high stiffness will result in the great change of surface shape of the mirror and the unqualified surface shape error produced. On the condition that the mirror surface shape error under temperature load and assembly error meet their index component, the stiffness of each part in the mirror subassembly is increased to the utmost to obtain the higher fundamental frequency of the mirror subassembly.

The higher the stiffness of the support structure, the smaller the displacement and the inclination angle of the mirror are. Furthermore, the mirror has better dynamic performance when the stiffness increase. The inclination angle of the mirror has great relation with support position. In addition, the mass of the mirror subassembly should be minimized in the premise of ensuring the performance indexes of the mirror subassembly. These four indexes are relatively easy to achieve.

On the contrary, the mirror surface shape error is relatively complex, on which there are many error sources that have an impact. Especially for the smaller surface shape error, it is necessary to carry out a targeted design for various error sources, which is more difficult. To clarify the errors that affect the mirror surface shape is required.

Four components affecting the mirror surface shape error are summarized after an in-depth research. They are the residual mirror

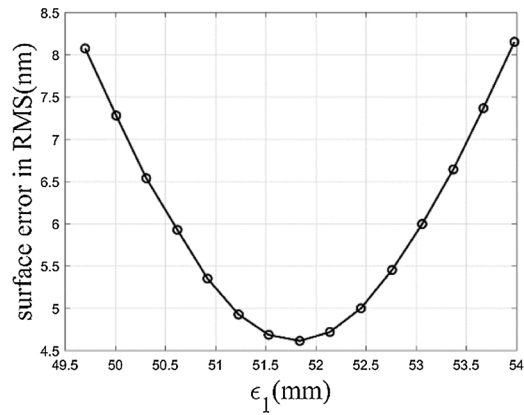


Fig. 3. The relation of mirror surface shape error and the distance between the rotation shaft and neutral plane in the optical axis direction.

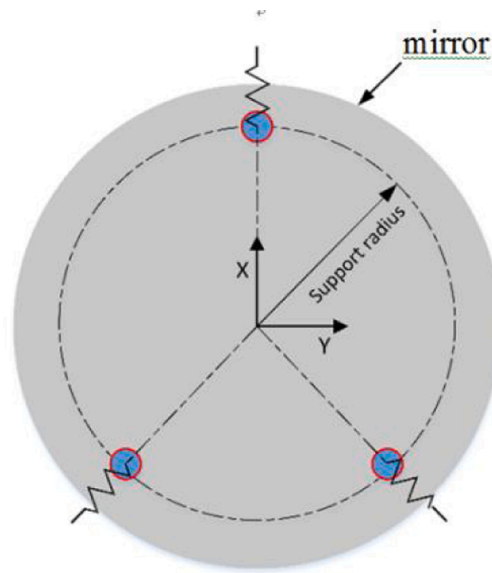


Fig. 4. Mirror subassembly with temperature load.

surface shape error caused by mirror finishing, the mirror surface shape error caused by the disappearance of gravity load, the mirror surface shape error caused by temperature load and the surface shape error caused by assembly [7].

3.2. Function decomposition

The space-based mirror with three point back support structure generally adopts “thin circular pie” structural form, whose radial stiffness is much greater than axial stiffness. The only difference between the assembly and test on the ground and the in-orbit application of the mirror subassembly is the presence or absence of a gravity load. The radial stiffness of mirror is large and the mirror is not sensitive to the gravity load when the mirror withstands the radial gravity load. So, the mirror supported by three points back structure generally keeps the optical axis in horizontal state when the mirror is assembled and tested on the ground. The force state of the mirror assembly under various loads is shown in Figs. 1–5.

The surface shape of the mirror will change because of the gravity load when the mirror is assembled and tested on the ground and the optical axis is in the horizontal state. The change of the surface shape is related to the mirror stiffness, axial support position and the flexible characteristics of the three flexible structures. The force state of the mirror subassembly in gravity load is shown in Fig. 1.

The design principle is improving the specific stiffness of the mirror, that is to maximize the stiffness of the mirror on the premise of meeting the mass requirements.

The surface shape error of the mirror under the gravity load is the most sensitive to the support position of the support structure in the direction of the optical axis. The weight moment of each part of mirror is balanced on the neutral plane of the mirror when the optical axis of the mirror subassembly is in the horizontal state. When the rotating shaft of the flexible structure coincides with the

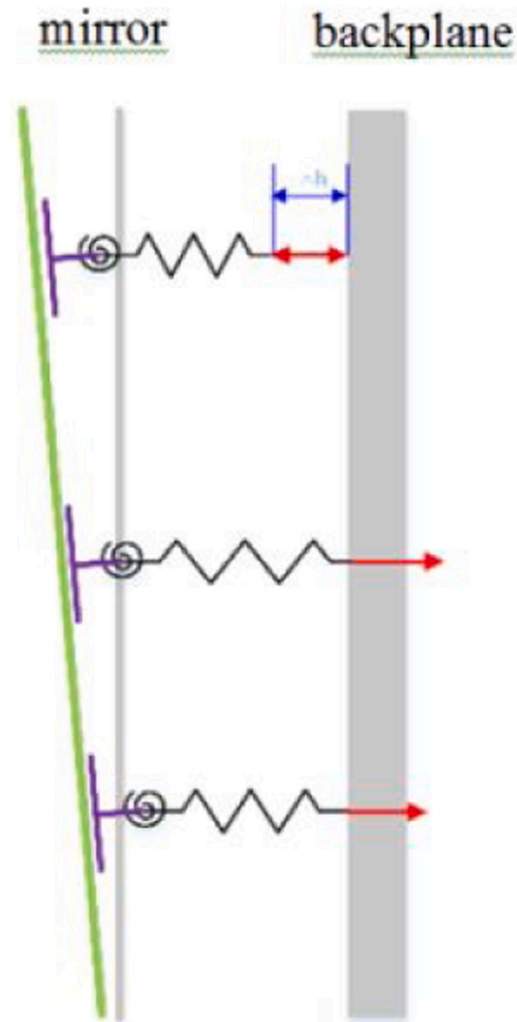


Fig. 5. Mirror subassembly with assembly error.

neutral plane of the mirror, the surface shape error of the mirror changes the least [8], as shown in Fig. 2.

For the surface shape error under the gravity load, the length of the cone sleeve can be adjusted to make the rotating shaft of the flexible structure coincide with the neutral plane of the mirror. The farther the rotating shaft is from the neutral plane of the mirror, the larger the surface shape error of the mirror caused by the gravity load will be, as shown in Fig. 3.

At present, the best method adopted to select the optimal axial support position is the finite element method, which makes the supporting rotating shaft coincident with the neutral plane of the mirror to ensure the surface shape error minimum.

The deformations of the three flexible structures on the back are same under the gravity load condition. The flexible structure is relatively soft in the whole mirror subassembly, especially for the mirror with relative larger stiffness to alleviate the surface shape error caused by the temperature load and assembly error. The mirror displacement is generated in the mirror under the gravity load. The deformations of the three flexible structures are same because of the larger stiffness of the mirror. In addition, the support forces of them are same, which is one third of the mirror weight respectively. The force state is shown in Fig. 1.

The mirror subassembly working in-orbit has to bear the temperature load with a certain amplitude even though the precise temperature control system is used. Because the material properties of the external frame on which the mirror subassembly installed and the mirror itself are different, the mirror will bear the thermal stress caused by the different coefficient linear expansion between these two materials under the temperature load, which will result in the variation of surface shape. So a flexible structure should be designed between mirror and the external frame to absorb and release partial thermal stress. Especially for a circular mirror supported by three points generally distributed uniformly at a circle on the mirror back, the radial flexibility of their flexible structures should be identical to relieve free expansion of the mirror and minimize the surface shape error effectively because of the symmetrical thermal load in a circular. The force state of flexible structure under temperature load is shown in Fig. 4.

Surface shape error caused by assembly error which mainly includes the machining error of the support structure and the flatness error of the connecting surface between the mirror subassembly and the flange on the external eframe. Part of these two kinds of error

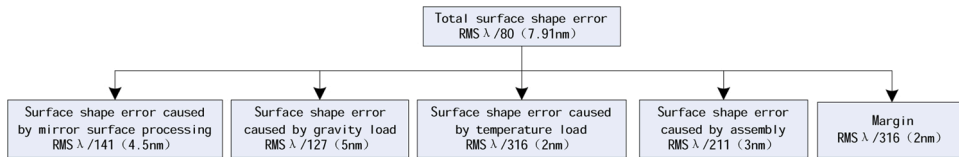


Fig. 6. Surface shape error allocation of mirror subassembly.

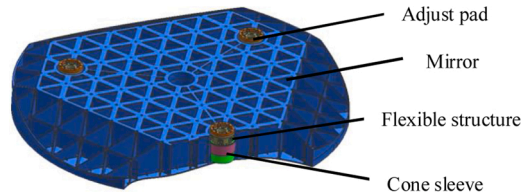


Fig. 7. Mirror subassembly.

act on the mirror surface directly. Stress and the surface shape error are produced on the surface of the mirror. So the flexible structures should be equipped in the direction of the surface shape error produced, which can convert the direct force on the mirror surface to the deformation energy of the flexible structure to reduce the deformation of the mirror surface. The assembly process of three-point back support is generally as follows:

- a) The cone sleeve is glued to the mirror body (3 groups).
- b) Lapping the connection surface between the cone sleeve and the flange on the support structure to ensure three surfaces coplanar.
- c) Install the support structure and lapping the connection surfaces between three supports and backplane or external frame to ensure three surfaces coplanar.
- d) Install mirror subassembly to the external frame.

According to the assembly process of the three-point back support structure, the machining error of the cone sleeve and support structure is finally transformed into the coplanar error of the connection surfaces of the three support points with flanges on external frame. The coplanar error can be controlled to the micron dimension by lapping. After the mirror subassembly is installed on the external frame, the coplanarity error which includes lapping residual and deformation of the connection flange face due to external force on the frame will affect the surface shape error of mirror indirectly. The mechanism of action of the flexible structure under assembly error is shown in Fig. 5.

The flexible structure generates elastic deformation and absorbs energy. However, which will bring the angle and the displacement of the mirror. Of course, the angle and displacement will be compensated back in the system integration stage.

The mechanism of surface shape error of the mirror has been studied and discussed from three aspects. Some necessary measures should be taken to eliminate the error sources that cause the surface shape error mentioned above when the support structure is designed.

3.3. Index allocation

The conclusion made from the above research is that the surface shape error is the most critical and hardest index of the mirror subassembly. In order to clarify the design target of support structure, the index allocation is carried out to quantify the surface shape error components which total index is 7.91 nm. As long as the actual error component is smaller than the corresponding allocated error component, the total surface shape error will be smaller than the total surface shape error index [9,10].

The relationship between the total surface shape error and its four components can be expressed as the error synthesis formula Eq. 1 as follows because they are approximately irrelevant.

$$\sigma = \sqrt{\sum_{i=1}^q \sigma_i^2 + \sum_{j=1}^s s_j^2} \tag{1}$$

Where σ_i is the random error and S_j is the single undetermined system error.

In consideration of the current optical machining ability for the mirror surface, machining precision for the mechanical parts and the assembly capacity of the mirror subassembly, the total surface shape error which is $\lambda/80(7.91 \text{ nm})$ is decomposed into five components (margin is included) shown in Fig. 6, which is useful and helpful to carry out a targeted design.

Except the allocated total surface shape error, the mirror displacement under the gravity load and the mass of mirror subassembly are also decomposed in order make the design simple.

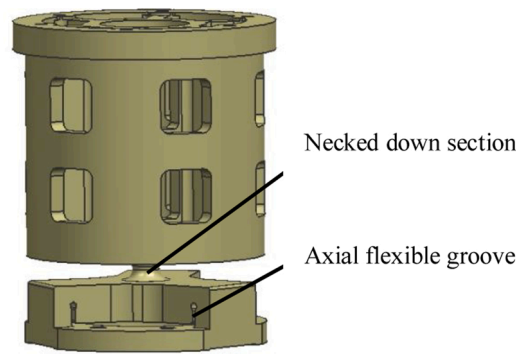


Fig. 8. Flexible structure.

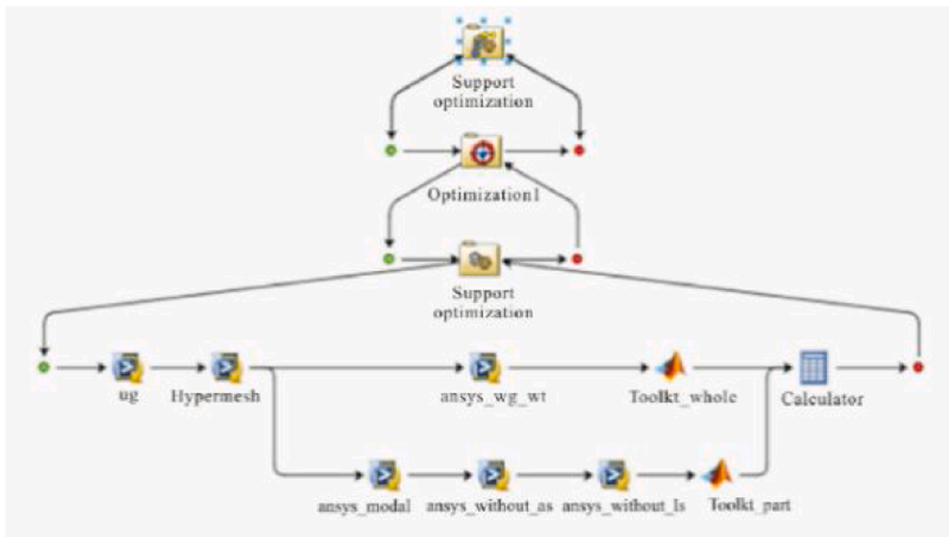


Fig. 9. Integrated simulation optimization links.

3.4. Structure design

The design constraints and objectives of the mirror subassembly with three-point back support structure are clarified after finishing the support principle analysis, error conclusion, function decomposition and index allocation [11–13]. The support scheme of mirror subassembly with three-point back support structure is shown in Fig. 7.

Mirror assembly includes mirror body, cone sleeve, flexible structure and adjusting pad.

SiC is widely used as material of mirror body to obtain smaller surface shape error, which has large specific stiffness, good dimensional stability and high lightweight ratio. The design target of the mirror body is to improve the specific stiffness.

Cone sleeve is a transition unit between the mirror body and the support structure which is the flexible structure. The material of flexible structure is usually titanium alloy with low density and stable performance. If the flexible structure directly adheres to the mirror, the mirror will bear thermal stress under the temperature load, worsen mirror surface shape, because there are larger differences between the linear expansion coefficient of the mirror and that of the flexible structure. Therefore, the cone sleeve with 4J32 material which linear expansion coefficient can be adjusted through changing the composition ratio of the material is glued to the mirror on one side, and connects to the flexible structure with screw fastening on other side, effectively avoiding thermal stress under the temperature load.

Flexible structure is the core component in the support scheme of mirror with three-point on the back, which directly determine the performance of the mirror subassembly. Therefore, the design of flexible structure should take full consideration of alleviating the thermal stress and assembly stress. Furthermore, on the base of principle analysis and function allocation, the flexible structure is shown in Fig. 8.

The adjusting pad is used to ensure that the mirror can locate in the theoretical position when the mirror assembly is installed to the external frame. The spatial position of the mirror is adjusted by lapping three pads.

The flexible structure is divided into rigid part and flexible part. Flexible part locates near the flange surface which is connected

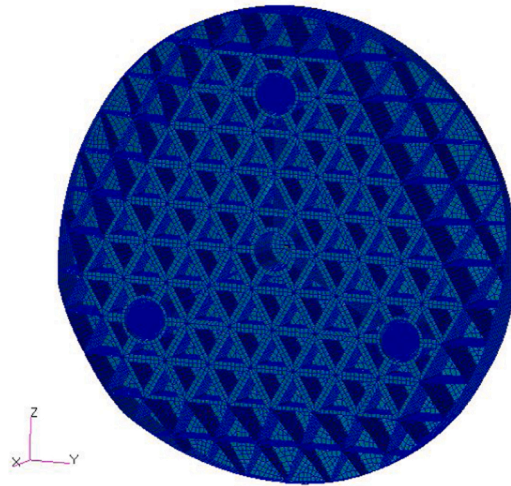


Fig. 10. Finite element model of mirror subassembly.

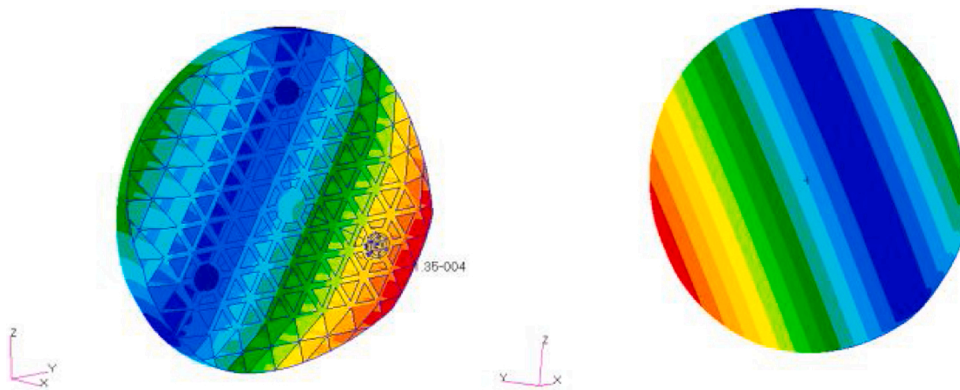


Fig. 11. The displacement cloud picture of mirror subassembly with coupling load.

with cone sleeve. Flexible parts includes axial flexible grooves and necked down section. Necked down section is used to simulate a universal joint. The axial flexible grooves include three groups, forming a three-leaf flexible structure, which are located in the form of 120 degree circular symmetrical layout, connecting to the necked down section on one end and to the connection flange surface with the cone sleeve. The axial groove is equivalent to a folded lamellar structure in radial distribution like a radial spring which principle is shown in Fig. 4. The radial folding layout of the shrapnel structure increases the radial length of the shrapnel and reduces the axial stiffness at the same time, which works with the simulated universal joint to weaken the influence to the mirror surface of assembly error. The working principle is shown in Fig. 5. The layout of the flexible structure in the mirror is shown in Fig. 1. The three groups of flexible structures are arranged around the rotation shaft of the mirror in the form of 120 degree circular symmetrical layout. The advantages of this three-leaf flexible structure for three-point support on the back are obvious, for the gravity load, the stiffness characteristics of the three flexible structure are the same, and for the thermal load, the stiffness characteristics of the thermal stress release direction, namely along the radial direction of 120° layout, are also the same. The flexible structure is applied to three-point support structures arranged symmetrically in the circumference on the mirror back, having the excellent ability to relieve the gravity load, the temperature load and the assembly error [14,15].

The surface shape error mainly includes four error sources. Surface shape errors caused by the temperature load and the assembly error are inversely proportional to the flexibility of the support structure. The larger the flexibility is, the smaller the surface shape error will be. However, the large flexibility will lead to the decrease of the fundamental frequency of the mirror subassembly and the increase of the dynamic stress of the flexible part. The integrated simulation optimization technology is necessary for design to solve the problem. The insight software integrated 3D modeling software and finite element software, and set up an integrated simulation optimization links as shown in Fig. 9.

The integrated optimization takes the minimum surface shape error caused by gravity load, temperature load and assembly error as the objective function to optimize the variables such as the flexible parameters including the diameter of necking down section, the length of necking down section, the width of axial flexible groove, the depth of the flexible groove and so on in the condition of

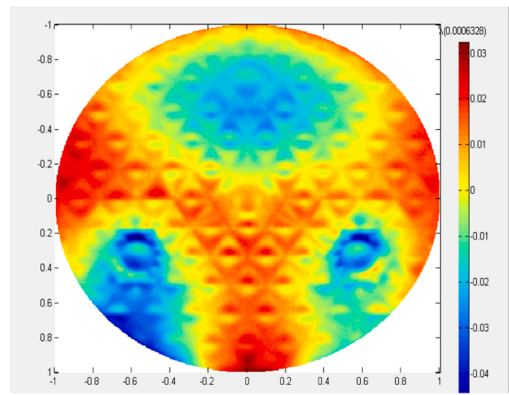


Fig. 12. The mirror surface shape cloud picture of mirror subassembly with coupling load.

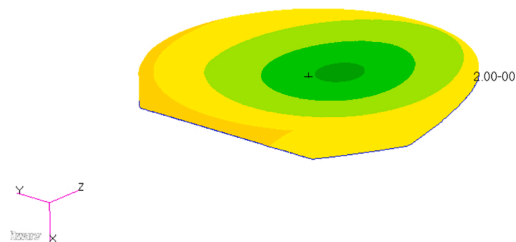


Fig. 13. The first natural vibration mode.

constraining the mass of mirror subassembly, fundamental frequency and dynamic stress. The optimization algorithm is adopted to optimize the flexible parameters of the support structure and obtain the mirror subassembly with the best performance.

4. Engineering analysis

Finite element simulation is widely used in engineering field, Which is mainly used for finding design defects, carrying out optimization design and performance evaluation of design schemes. Given the rules of various experiments of space-based mirror subassembly, the coupling statics simulation with force, temperature and assembly error and dynamic simulation are carried out [16].

The hexahedral solid element is used to build the finite element model of the support structure and the quadrangle shell element is used to build the finite element model of the mirror, which is shown in Fig. 10.

4.1. Coupling statics analysis

The finite element analysis is carried out to verify the static performance of the mirror subassembly whose optical axis is in the horizontal direction under the coupling load including the gravity load (1 g), temperature load(4°C), and assembly error (0.05 mm coplanarity error on the connection flange faces of three flexible structure with the external frame). The result is that the surface shape error of mirror body is 5.9 nm. The displacement cloud picture of mirror subassembly under coupling load is shown as Fig. 11. The mirror surface shape error cloud picture is shown in Fig. 12. When the gravity load (1 g) is applied alone, the surface shape error of the mirror subassembly is 4.83 nm, the mirror displacement in the gravity direction is 0.013 mm and the inclination angle is 0.08". When 4°C temperature load is applied alone, the surface shape error of the mirror subassembly is 1.89 nm. When a coplanarity error about 0.05 mm is applied alone, the surface shape error of the mirror subassembly is 2.73 nm. All the analysis results meet the design requirements.

4.2. Dynamic analysis

Mirror subassembly may be out of work because of the vibration, impact and overload in the process of transport and emission. Modal analysis, sine vibration response analysis and random vibration response analysis are conducted to verify that the mirror subassembly have a high enough stiffness and strength, a reasonable dynamic stiffness and dynamic response caused by the external excitation and ensure the dynamic stress less than yield limit of the materials applied [17,18].

The result of modal analysis shows that the fundamental frequency of the mirror subassembly is 128 Hz that is much higher than the design target of 120 Hz, which indicates that the mirror subassembly has a sufficiently high dynamic stiffness. The fundamental frequency mode is the rotation around the X-axis (optical axis), as shown in Fig. 13.

Table 1
The sine vibration test condition of the mirror subassembly.

| Direction | X | | Y、Z | |
|----------------|---------------|-----------|---------------|-----------|
| | frequency(Hz) | magnitude | frequency(Hz) | magnitude |
| Parameters | 5~10 | 13.8mm | 4~9 | 1.48g |
| | 10~15 | 5.5g | 9~31 | 7.5g |
| | 15~31 | 7.5g | 31~80 | 4.0g |
| | 31~80 | 5.5g | 80~100 | 2.5g |
| | 80~100 | 2.8g | | |
| Scan frequency | 2oct/min | | | |

Table 2
The random vibration test condition of the mirror subassembly.

| Direction | X | | Y | | Z | |
|------------------------------|---------------|-------------|---------------|--------------|---------------|--------------|
| | frequency(Hz) | magnitude | frequency(Hz) | magnitude | frequency(Hz) | magnitude |
| Parameters | 10~20 | +6dB/oct | 10~20 | +6dB/oct | 10~20 | +6dB/oct |
| | 20~125 | 0.075 g2/Hz | 20~103 | 0.0315 g2/Hz | 20~105 | 0.0315 g2/Hz |
| | 125~185 | 0.01 g2/Hz | 103~165 | 0.004 g2/Hz | 105~165 | 0.004 g2/Hz |
| | 185~200 | 0.075 g2/Hz | 165~200 | 0.0315 g2/Hz | 165~200 | 0.0315 g2/Hz |
| | 200~2000 | -3 dB/oct | 200~2000 | -3 dB/oct | 200~800 | -3 dB/oct |
| Total rms acceleration(grms) | 6.69g | | 4.31 g | | 4.33g | |
| Testing time(min) | 2 | | | | | |

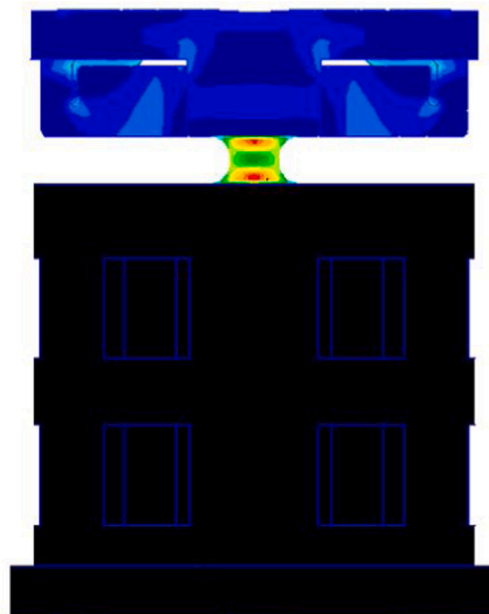


Fig. 14. The stress distribution of flexible structure under sine vibration.

In the mechanical test of the whole space remote sensor, the test sensor is pasted at the installation position of the mirror subassembly on the space remote sensor. The data from test sensor can be used as mechanical inputs of the mirror subassembly. The input conditions of the mechanical test for sine vibration response analysis and random vibration response analysis are shown in [Tables 1 and 2](#). Through sine vibration response analysis and random vibration response analysis, the response magnification of mirror subassembly and the dynamic stress at the flexible part of mirror subassembly can be predicted.

The results of sine vibration response analysis shows that the maximum stress occurs in the necking down section of the flexible structure, whose X Y Z components are 59.5 MPa, 114 MPa and 122Mpa respectively. The maximum stress position is shown in [Fig. 14](#). The vibration stress curve of most dangerous position in the z direction is shown in [Fig. 15](#). The maximum magnification in X direction is 2.47 times at 80 Hz, in Y direction is 2.14 times at 100 Hz, and in Z direction is 2.18 times at 100 Hz. The acceleration response curve of sine vibration in x direction is shown in [Fig. 16](#).

The result of random vibration response analysis indicates that the most dangerous position locates in the necking down section of



Fig. 15. Dynamic stress curve of the most dangerous position of the flexible structure in z direction.

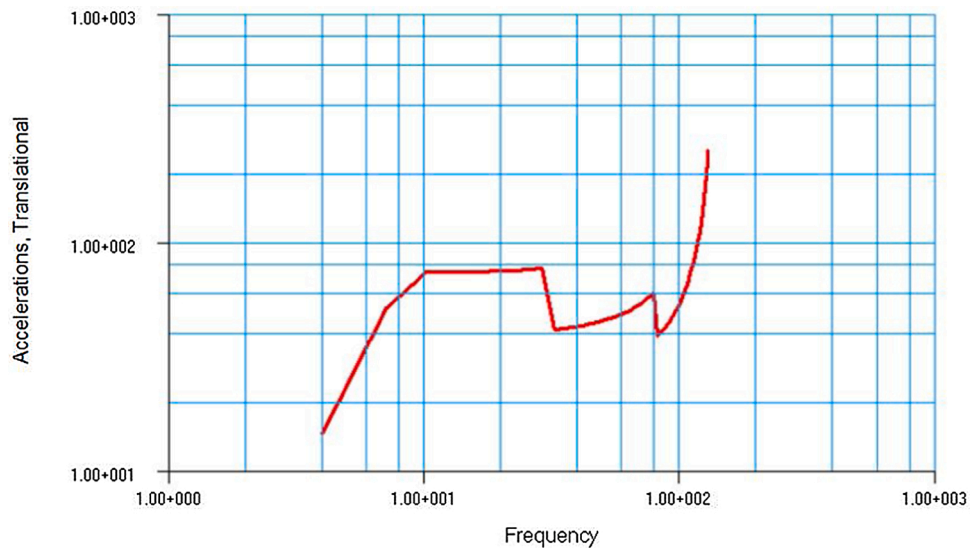


Fig. 16. The sine vibration acceleration response curve in z direction.

the flexible structure, whose maximum stress in X direction is 159Mpa, in Y direction is 234Mpa and in Z direction is 286Mpa. The stress distribution state of flexible structure in random vibration in Z direction is shown in Fig. 17. The response amplification of the total rms acceleration in X direction is 1.01 times, in Y direction is 1.24 times and in Z direction is 1.59 times. The response curve of the random vibration acceleration in Z direction is shown in Fig. 18.

5. Experimental verification

The mirror is processed in the form of a single mirror before the mirror surface is modified by Si layer. After the mirror surface is modified, the cone sleeve is adhered to the mirror on one side and is connected to the flexible structure on other side with screw fastening forming the mirror subassembly. From now on, the mirror is processed in the form of mirror subassembly. Process the mirror surface to the required surface shape error and then carry out the film coating. The processing cycle of mirror surface is long which is about 2 years, in order to verify in advance the statics performance without mirror surface shape error and dynamic performance, expose the design defects, an equal-scale test article of mirror subassembly which mirror's material is aluminum having the equal inertia and mass with the real SiC mirror and which support structures are the actual ones is made to carry out the static and dynamic test.

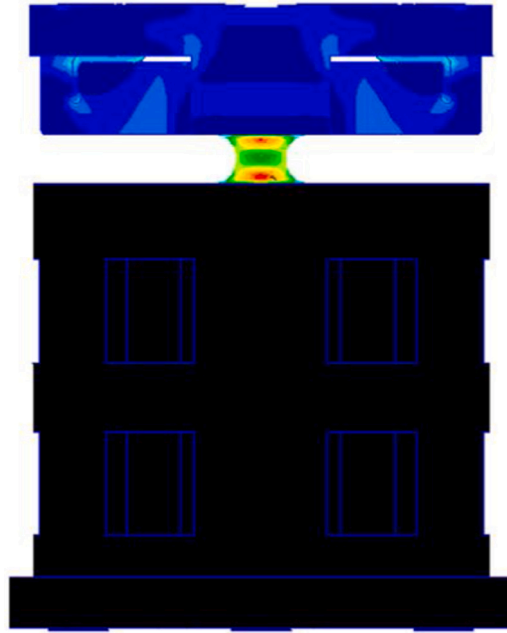


Fig. 17. The stress distribution of flexible structure under the random vibration.

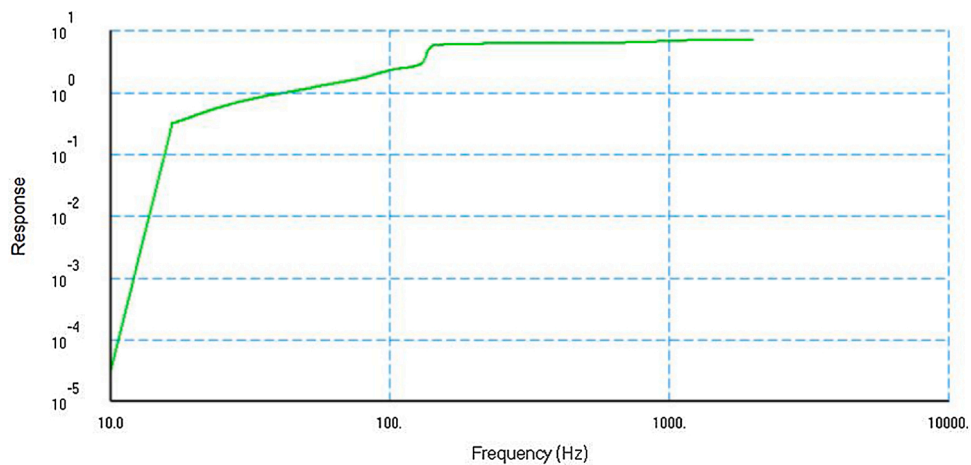


Fig. 18. The random vibration acceleration response curve in z direction.

5.1. Test of displacement and inclination angle

Digital display dial indicator and goniometer are employed to test the displacement and inclination angle of the mirror respectively according to the requirements. The mirror displacement test is shown in Fig. 19 and the inclination angle test is shown in Fig. 20. The post-processed test results indicates that mirror displacement is 0.012 mm and the inclination angle is 0.9" under gravity load (1 g), which are better than the design indexes.

5.2. Mechanical test

The mechanical vibration test is carried out on the mirror subassembly to test the dynamic performance of the mirror subassembly. Fig. 21 shows the mechanical vibration test environment. Sine vibration test and random vibration test are carried out in X, Y and Z directions. The test results indicate that the fundamental frequency of the mirror subassembly is 131.5 hz which is basically consistent with the mechanical simulation results. The response amplification of sine vibration in X, Y and Z directions are 2.51 times, 2.12 times and 2.25 times respectively, and the dynamic stress are 62Mpa, 110Mpa and 131Mpa respectively. Fig. 22 shows the sine vibration response curve in z direction.

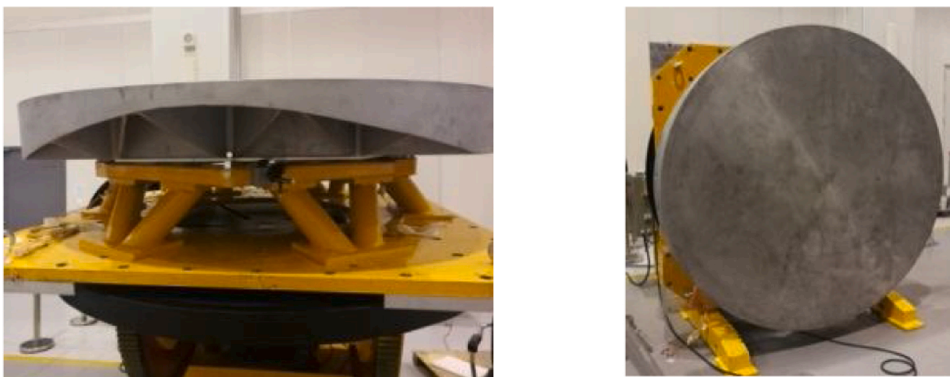


Fig. 19. Test of mirror displacement.



Fig. 20. Test of mirror inclination angle.



Fig. 21. Test of mechanical vibration.

The total rms amplification of random vibration in X, Y and Z directions are 1.11 times, 1.33 times and 1.65 times respectively, and the maximum dynamic stress are 150Mpa, 214Mpa and 262Mpa respectively. Fig. 23 shows the random vibration response curve in z direction.

6. Installation and adjustment

Based on the theoretical study of mirror subassembly supported by three points on the back, it is concluded that the surface shape error of the mirror subassembly are mainly caused by the mirror machining residuals, the disappearance of gravity load, the temperature load and the influence of assembly error. Mirror machining residuals are controlled by optical machining. The problems of gravity load disappearance, temperature load and assembly error depend on the mechanical design and assembly technology.

The surface shape error introduced by the temperature load depends on the temperature control capability of the thermal control system and the flexibility of the flexible structure, and has nothing to do with the assembly technology.

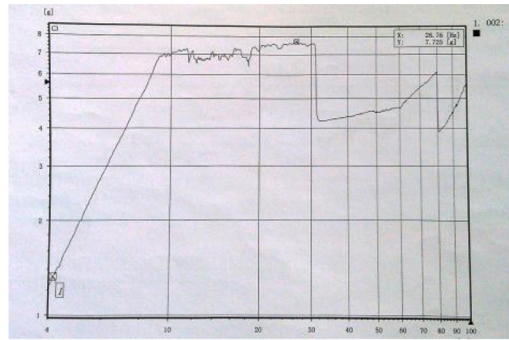


Fig. 22. The sine vibration acceleration response curve in z direction.

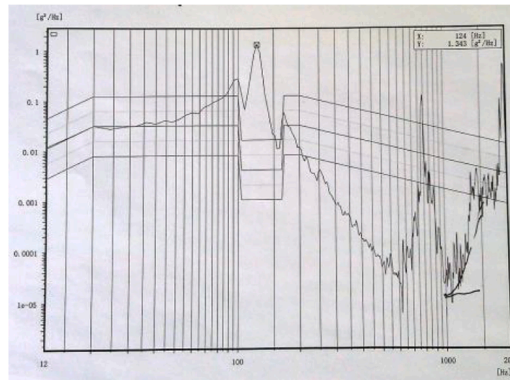


Fig. 23. The random vibration acceleration response curve in z direction.

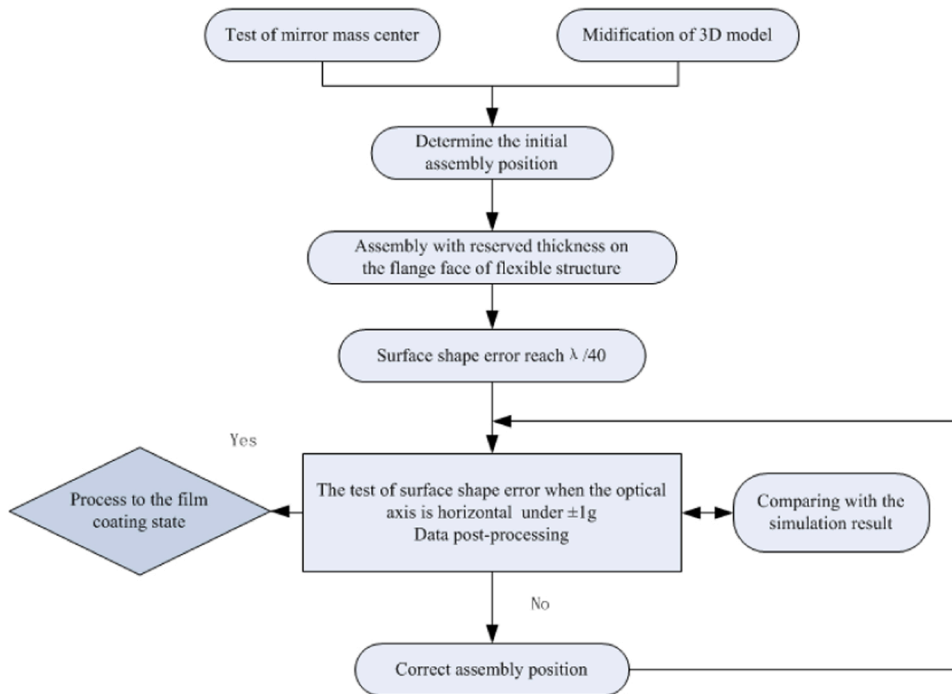


Fig. 24. The flow chart of assembly technology with small surface shape error.



Fig. 25. The geometric parameters measurement of the mirror.



Fig. 26. The test of mirror's mass center.

The mirror surface shape error introduced by the assembly error depends on the assembly technology, the influence factor is clear and the solution is mature. During assembly, it is necessary to reduce the coplanarity error of each flange face to lower the surface shape error caused by assembly.

For the mirror subassembly which optical axis is in the horizontal direction in test, installation and adjustment, the surface shape error introduced by the disappearance of gravity load depends on the specific stiffness of the mirror and the position of support structure in the optical axis direction. The design goal of the mirror subassembly is to obtain a mirror with high enough specific stiffness and the theoretical optimal assembly position of the support structure in the optical axis direction in the mirror. The surface shape error introduced by the disappearance of the gravity load is sensitive to the alignment error between mirror's neutral plane and the rotating shaft of the flexible structure. So it is very important to find the mirror's neutral plane, especially for the mirror which surface shape error index is very small. Therefore, a segmented metering assembly technology with small surface shape error for a space-based large-aperture mirror with three-point support on the back is proposed [19,20]. The detailed flow chart of assembly technology is shown in Fig. 24.

The key of the assembly technology with small surface shape error lies in exactly ensuring that the neutral plane of the mirror coincides with the rotating axis of the flexible support structure [19]. Therefore, it is important to know the position of neutral plane of the mirror, but for the complex lightweight mirror, neutral plane of the mirror is immeasurable which related to the mass distribution of the mirror. The rotating shaft of the support structure is expected to coincide with the neutral plane of the mirror, so it is necessary to detect the geometric parameters of the actual mirror, then modify the 3D model, carrying out a simulation calculation with the modified 3D model for the neutral plane of the mirror. The geometrical parameters detection of the mirror are shown in Fig. 25.

Also the geometric parameters measurement of the actual mirror have the measurement error, so the position of neutral plane obtained with the modified 3D model which have the geometric parameters measurement error also have the error. The above position error is uncertain, because the neutral plane can not be detected with test tools or equipment. Luckily, the mass center of mirror can be measured with a tester of centroid and rotation inertia which test precision is ± 0.5 mm, the deviation between the mass center of the actual mirror and the modified 3D mirror model can be used to compensate the deviation between the neutral plane of the actual mirror and the modified 3D mirror model. The testing process of the center of mass is shown in Fig. 26.

After the test of mirror's mass center and the modification of 3D mirror model, compare the measured mass center of actual mirror with the simulative mass center of the modified 3D mirror model.

Assuming that the distance of the measured mass center of actual mirror from mirror back is L_1 , the distance of the simulative mass center of the modified 3D mirror model from mirror back is L_2 , the distance of the optimal position obtained through simulation analysis with the modified 3D mirror subassembly model where the rotating shaft of flexible structure lies in optical axis direction from mirror back is L_3 , that is to say, the simulated neutral plane with the modified 3D mirror model from back is L_3 . L_1 and L_2 are not equal, because of the geometric parameters measurement error, so the deviation between the neutral plane of the actual mirror and the modified 3D mirror model also exists, which is about $\Delta = L_1 - L_2$. Then the distance of the neutral plane from mirror back is $L_3 + \Delta$,

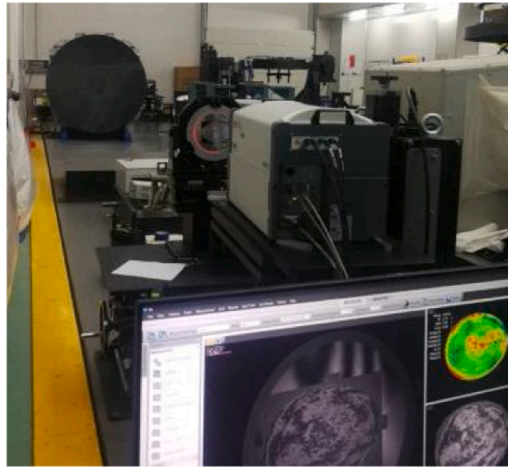


Fig. 27. The optical path of surface shape error test.

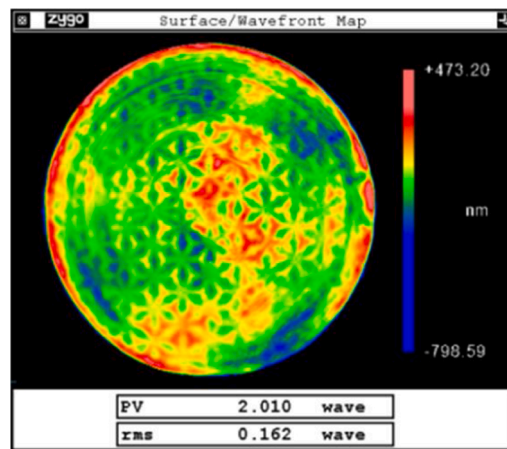


Fig. 28. The surface shape of mirror subassembly.

where is the best position the rotating shaft of flexible structure lies in the actual mirror in the optical axis direction. When the surface shape error of mirror without support structure is 0.164λ , the flexible structure is assembled with the mirror. After the assembly, the optical path of the surface shape error test is set up. The surface shape error is tested in the form of mirror subassembly as shown in Fig. 27, and the surface shape error is 0.162λ without change as shown in Fig. 28.

The test precision of the tester of centroid and rotation inertia is ± 0.5 mm, so the above best installation position still exists a deviation from the actual best position which is about ± 0.5 mm. When the surface shape error of mirror subassembly is smaller than $\lambda/40$, test the surface shape error with the optical axis horizontal around optical axis at 0° and 180° , obtaining surface shape error under 1 g gravity load by post-processing with the two surface shape error under the gravity load of ± 1 g. If the surface shape error is equal to the simulation result, it is considered that the rotating shaft of flexible structure coincides with the neutral plane of mirror. Otherwise, there is a slight deviation between the actual support position and the optimal support position. By comparing the measured surface shape error and surface shape distribution trend from post-processing with the surface shape error and surface shape distribution trend from simulation analysis, obtain the deviation magnitude and direction of the rotating shaft of flexible structure and neutral plane, correct the installation position by having a lapping the flange face with reserved thickness of flexible structure, ensure that the surface shape error is the minimum which is approximately equal the theoretical design value.

7. Conclusion

In order to meet the requirements of small surface shape error and high stability of the mirror subassembly of space remote sensor, the support principle of the three-point support on the back of the mirror is studied, and the sources of the surface shape error is analyzed in detail, and the corresponding design is carried out for the error sources. A flexible support structure is obtained which can alleviate various error sources simultaneously. Simulation analysis and experimental verification are carried out for mirror

subassembly. The surface shape error under theoretical coupling load is $\lambda/107$ ($\lambda = 632.8$ nm), and the final surface shape error of the mirror subassembly is expected to be better than $\lambda/80$. The mirror displacement is 0.013 mm, which is less than 0.015 mm of the index. The inclination angle is $0.9''$, which is less than $2''$ of the index. The fundamental frequency is 128 Hz, which is larger than the design requirement of 120 Hz. The mass of the mirror subassembly is 305 kg, which is less than the design requirement of 310 kg. The maximum dynamic stress in sine vibration and random vibration is 286 MPa, which is far less than the yield limit of the selected material. A set of segmented metering assembly technology with a smaller surface shape error on a large-aperture mirror is formed and applied to a 2 m-diameter mirror subassembly.

Funding

National Natural Science Foundation of China (NSFC) (11703027).

Declaration of Competing Interest

The authors declare that there are no conflicts of interest.

References

- [1] J. Shao, Investigation on supporting structure of spacial reflector, *Infrared* 27 (4) (2006) 36–41.
- [2] E. Sein, Y. Toulemont, J. Breyse, P. Deny, D. Chambure, T. Nakagawa, M. Hirabayashi, A new generation of large SiC telescopes for space applications, *Proc. SPIE* 5528 (2004) 83.
- [3] Zeng Y Q, Fu D Y, Sun J W, et al., "Summary of support structure patterns of large mirror for Space remote sensor". *Spacecraft Recovery and Romote*.
- [4] Jiao Shi-ju, Achievement and prospect of satellite remote sensing technology in china, *Proc. SPIE* 3505 (1998) 26–30 (S0277-786X).
- [5] L. Fan, Research on the Lightweight Design and Support of 2m-SiC Primary Mirror for Ground-Based Telescope, University of Chinese Academy of Sciences, Changchun, 2013.
- [6] J. Wangk, Research on the Lightweight Design and Compound Support of the Large-Aperture Mirror for Space-Based Telescope, University of Chinese Academy of Sciences, Changchun, 2016.
- [7] Wang Kejun, Dong Jihong, Wang Xiaoyu, Chi Chunyan, Design of frame type support structure for space-based rectangular convex mirror tested on the back, *Opto-Int. J. Light Electron. Opt.* 212 (2020) 164673.
- [8] Keith B. Doyle, Victor L. Genberg, Gregory J. Michels, *Integrated Optomechanical Analysis*, SPIE PRESS, 2012.
- [9] Y.P. Cui, X. He, K. Zhang, et al., The support design of reflected mirror from the principle of three points supported, *Opt. Instrum.* 34 (6) (2012) 56–61.
- [10] F. Yang, G.J. Liu, Q.C. An, Error allocation of opto-mechanical system for large aperture telescope based on structure function, *Opt. Precis. Eng.* 23 (1) (2015) 119–221.
- [11] R.W. Besuner, K.P. Chow, S.E. Kendrick, S. Streetman, Selective reinforcement of a 2m-class lightweight mirror for horizontal beam optical testing, *Proc. SPIE* 7018 (2008), 701816.
- [12] Z.S. Wang, Y. Zhai, G. Mei, et al., Design of flexible support structure of reflector in space remote sensor, *Opt. Precis. Eng.* 18 (8) (2010) 1833–1841.
- [13] N.B. Zhu, Research on the Design of the Supporting Structure of Lightweight Mirror, University of Chinese Academy of Sciences, Chengdu, 2016.
- [14] X. Wang, Optimal Research on 800mm Reflect Mirror and Its Support Structure of Space Camera, University of Chinese Academy of Sciences, Xian, 2014.
- [15] S.H. Li, Y.J. Guan, H.W. Xin, et al., Lightweight design and flexible support of large diameter mirror in space camera, *Laser Infrared* 47 (11) (2017) 1422–1427.
- [16] H.D. Chen, Y.H. Chen, T. Shit, et al., Lightweight and mounting design for primary mirror in space camera, *Infrared Laser Eng.* 43 (2) (2014) 535–540.
- [17] Z.X. Li, Analysis and test on the response of primary mirror flexure under random vibration, *Infrared Laser Eng.* 43 (s) (2014) 101–107.
- [18] R. Goullioud, D.A. Content, G.M. Kuan, J.D. Moore, Z. Chang, E. T.Sunada, C.A. Powell, Wide Field Infrared Survey Telescope[WFIRST]: telescope design and simulated performance, *Proc. SPIE* 8442 (2012) 84421U.
- [19] P.R. Yoder, *Opto-Mechanical Systems Design*, China Machine Press, Beijing, 2008.
- [20] P. Bely, *The Design and Construction of Large Optical Telescopes*, Springer, 2003.